1
Introduction

2
Results

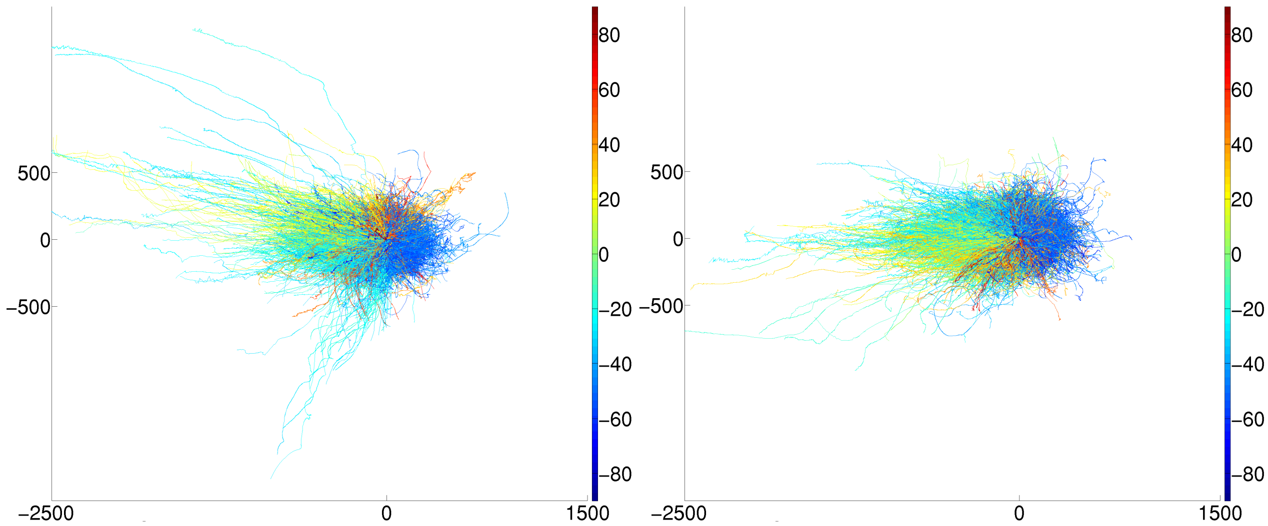

Figure 2.1: Left: anticyclones. Right: cyclones. Color represents *birth-latitude*. Thickness (hardly noticable) represents IQ. Data is from a predecessor run to POP-7day-MII .

The short time frame and limited computational resources allowed for only a few complete global runs over the available data. It was therefor critical to carefully choose which method/parameters to use in order to maximize the deducible insight from the results. For best comparability of the results with each other it was decided to agree on one complete set of parameters as a basis (**??**), which would then be altered at key parameters. The first run is an attempt to reproduce the results from **?**. The SSH-data for this run is therefor that of the Aviso product. This method will be called MI.

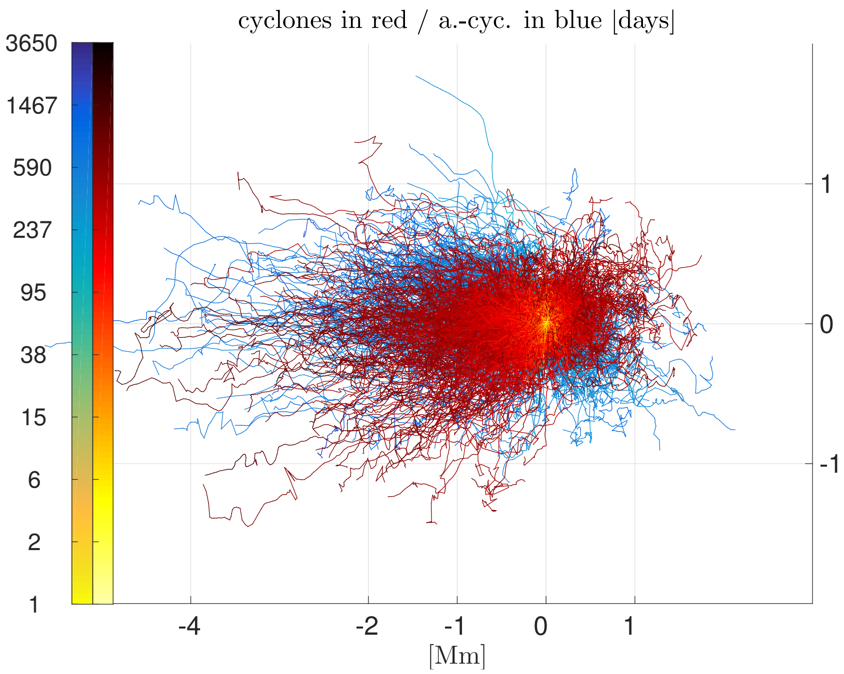

Figure 2.2: Aviso -MI: Basleline-shifted *old* tracks. Tracks younger than 500*days* **TODO: !** omitted.

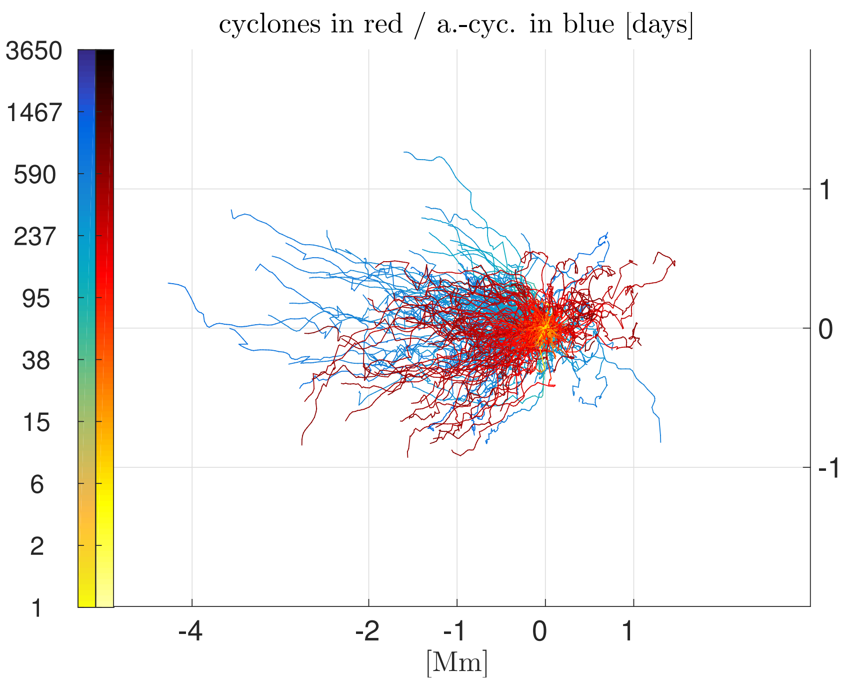

Figure 2.3: Aviso -MII: Basleline-shifted *old* tracks. Tracks younger than 500*days* **TODO: !** omitted.

THE second run (MII) is equivalent, except that this time the alternative IQ-based shape filtering method from TODO ref and the slightly different tracking-filter as described in **TODO: ref**

are used. MIIis then fed with 7-day time-step POP data as well.

TO INVESTIGATE what role spatial resolution plays, the POP data was remapped to that of the Aviso data and fed to the MImethod.

FINALLY , to investigate the effects of resolution in time, an MII-1-day-time-step run over POP data was executed. **TODO: POP-1day-MII-Southern-Ocean**

START AND END DATES were fix for all runs as the intersection of availability of both data sets.

TODO: Cheltons idendity check takes Leff?

time frame	1994/01/05 till 2006/12/27
scope	full globe ($80S$: $80N$ $180W$: $180E$)
Aviso geometry	$641x1440$ true Mercator
POP geometry	$2400x3600$
contour step	0.01
thresholds	[all SI]
max σ/L_R	4
min L_R	20e3
min IQ	0.55
min number of data comprising found contour	8
max(abs(Rossby phase speed))	0.2
min amplitude	0.01

Table 2.1: Fix parameters for all runs. **TODO: SI**

Box 1: Method MI

The concepts used in this method are mostly based on the description of the algorithm described by **?** and all parameters are set accordingly. Basically MIis a modification of MII(which was completed first), with the aim to try to recreate the results from **?**. It differs from MIIin the following:

- **detection**

  As mentioned in TODO ref, the approach by **?** is to avoid overly elongated objects by demanding:

  - high latitudes

    The maximum distance between any vertices of the contour must not be larger than $400km$ for $|\phi| > 25°$.

  - low latitudes

    The $400km$-threshold increases linearily towards the equator to $1200km$.

- **tracking**

  The other minor difference to MIIis in the way the tracking algorithm flags eddy-pairs between time-steps as sufficiently similar to be considered successful tracking-candidates (see TODO ref). In this method an eddy B from time-step $k + 1$ is considered as a potential manifestations of an eddy A from time-step k as long as both - the ratio of amplitudes (with regard to the mean of SSH within the found contour) and the ratio of areas (interpolated versions as discussed in TODO ref) fall within a lower and and an upper bound.

Box 2: Method MII

The purpose of this variant is basically to test the conceptually very different idea of the IQ-technique to test the shape of found contours for sufficiently eddy-*typical*. It also uses a slightly different tracking algorithm.

- **detection**

  The IQ-method. See **??** and **??**.

- **tracking**

  Conceptually similar to MI, it is again vertical and horizontal scales that are compared between time-steps. Preferring a single threshold-value over one upper and one lower bound, a parameter ξ was introduced that is the maximum of the two values resulting from the two ratios of amplitude respective σ, where either ratio is -if larger- its reciprocal in order to equally weight a decrease or an increase in respective parameter. In other words: $\xi = \max\left([\exp|\log R_\alpha|\ ;\ \exp|\log R_\sigma|]\right)$, where R are the ratios. **TODO: this has been explained twice now..**

2.1 *MI - 7 day time-step - Aviso*

THE RESULTS from the MI-method are special in that they feature many long-lived eddies (see **??????**), some of which travelled more than 4000 km west. Tracks were recorded throughout the entire world ocean with the only exeptions being an approximately 20°-wide stripe along the equator. The highest count of unique eddies is along the Antarctic Circumpolar Current [1] with counts of more than 60 individual eddy-visits per $1° \times 1°$-cell. Further eddy-rich regions are the western North-Atlantic throughout the Gulf-Stream and North-Atlantic Current, *Mozambique eddies* (**?**) at 20° South along the Mozambique coast, along the Agulhas Current and south of the Cup

[1] abbreviated ACC from here on.

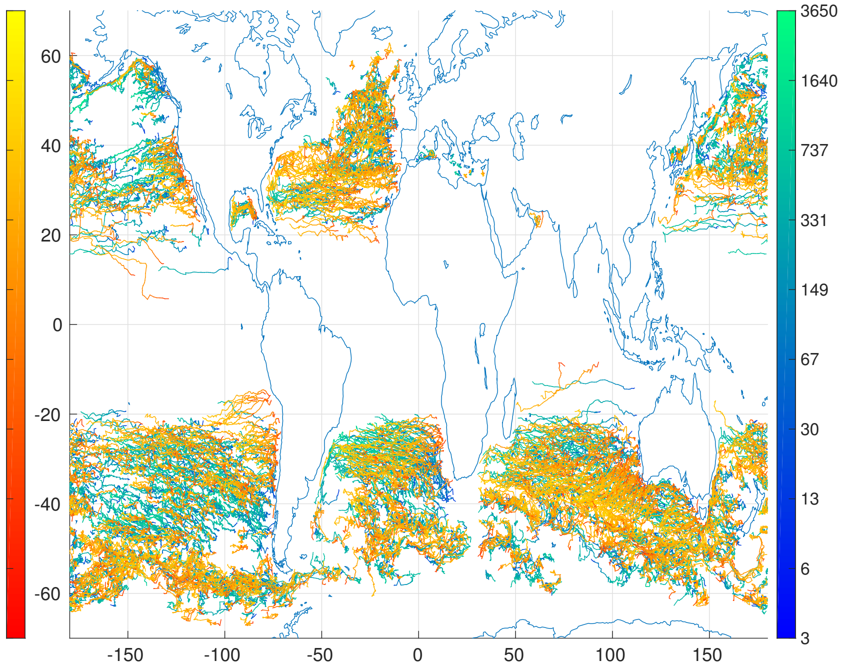

Figure 2.4: MI: anti-cyclones ind red. Tracks younger than 1a omitted for clarity.

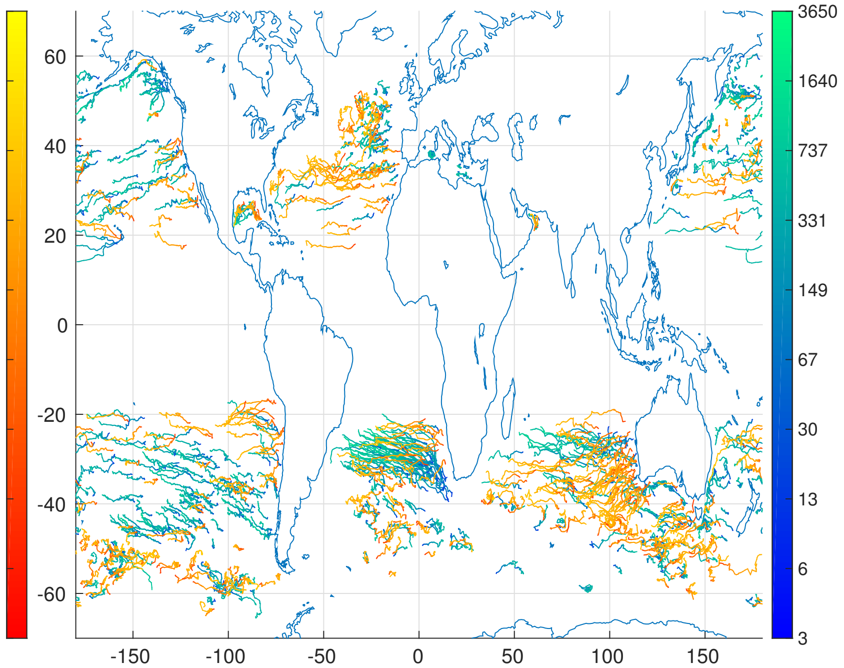

Figure 2.5: MII: anti-cyclones ind red. Tracks younger than 1a omitted for clarity.

of Good Hope at $\sim 40°$, along the coasts of Brazil, Chile and all along the Eastern, Southern and Western coasts of Australia (see **??**).

Eddies appear and disappear throughout the world ocean. For long-lived solid eddies there is a tendency to emerge along western coasts (see **??**).

The scale σ of tracked eddies is similar to that in **?**, yet generally smaller in high latitudes and slightly larger in low latitudes (see **??**). It is larger than the first-mode baroclinic Rossby Radius by factor of at least 2 and its meridional profile appears to be separable into two different regimes; one apparently linear profile in low latitudes and a steeper one equator-wards of $\sim |15°|$. Regionally, locations of high mesoscale activity appear to correlate with smaller eddy-scales (see **??**).

The eastward zonal drift speeds are slightly slower than the first-mode baroclinic Rossby-Wave phase-speed and agree well with the results from **?**. Propagation is generally west-wards except for regions of sufficiently strong eastward advection as in the ACC and North Atlantic Current (see **????**).

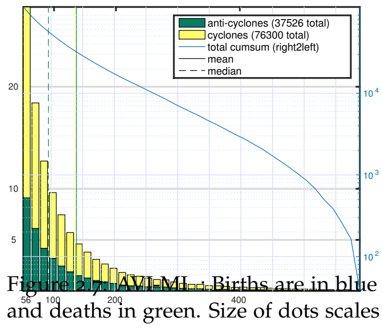

Figure 2.6: AVI-MI : Final age distribution. x-axis: [days], Left y-axis: [1000]

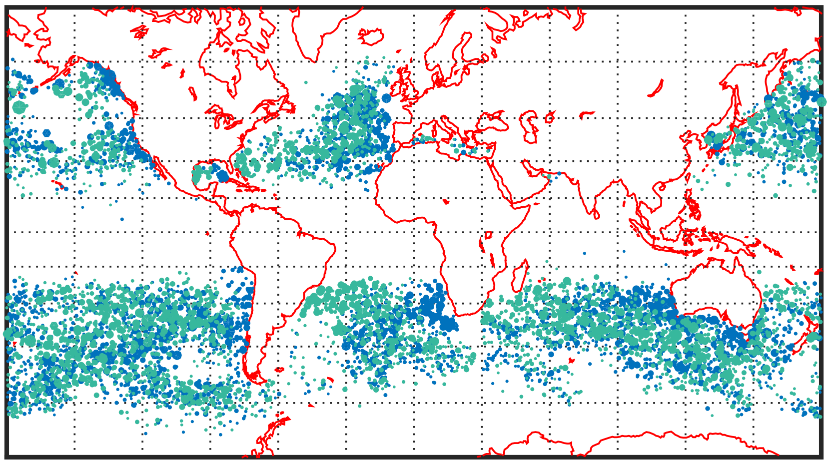

Figure 2.7: AVI-MI : Births are in blue and deaths in green. Size of dots scales to age squared. Only showing tracks older than one year.

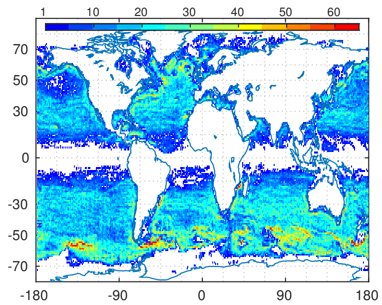

Figure 2.8: AVI-MI : Total count of individual eddies per 1 degree square.

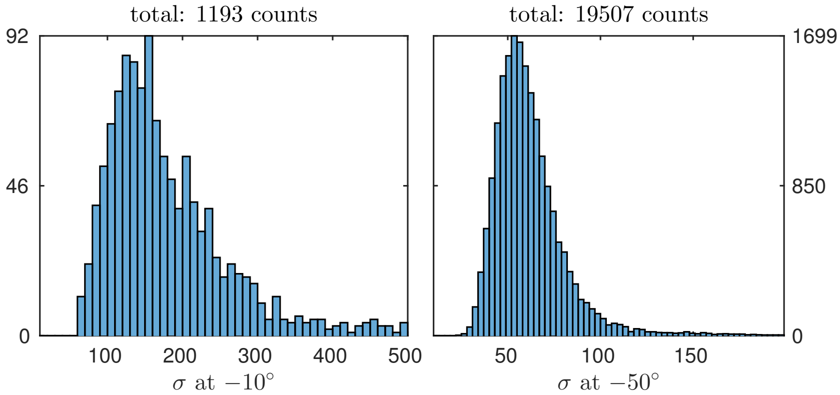

Figure 2.9: AVI-MI : σ[km]

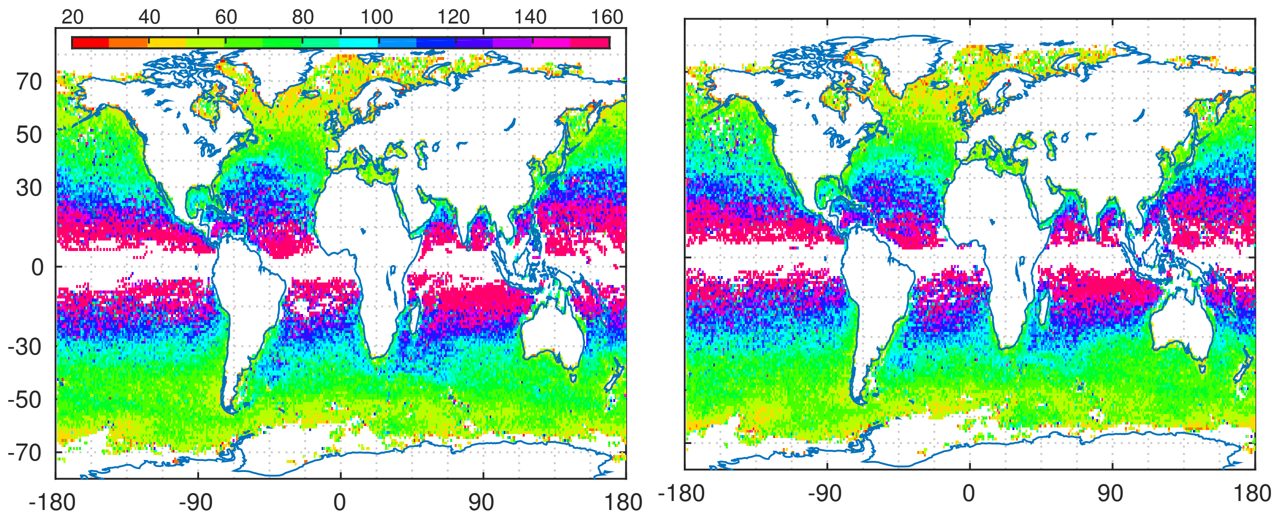

Figure 2.10: AVI-MI : σ[km]

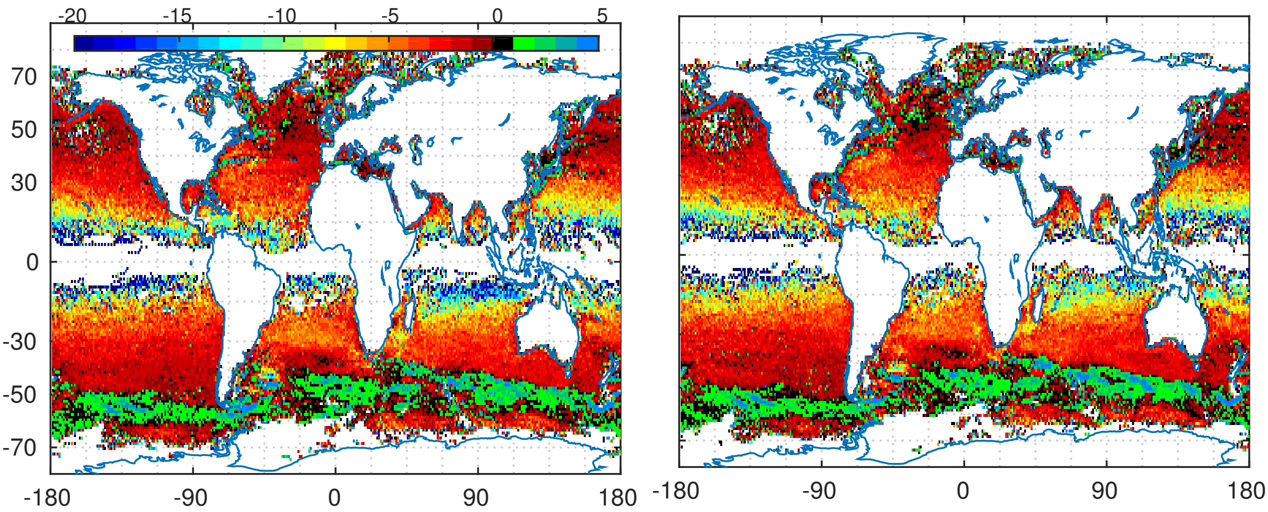

Figure 2.11: AVI-MI : zonal translational speed [cm/s]

2.2 *MII - 7 day time-step - Aviso*

The IQ-based method results in approximately the same total amount of tracks as the MI-method used in **??** (see **????**). The difference is that tracks here are generally much shorter, meaning that less eddies are detected at any given point in time.

The scale σ is now smaller than that from **?** for all latitudes in zonal-mean as well as median.

Westward drift speeds are almost identical to those in **??**.

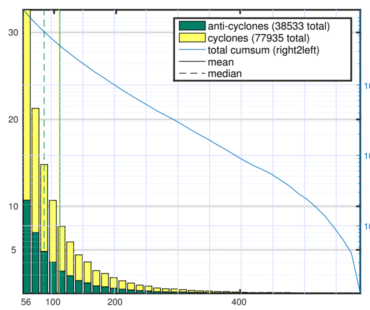

Figure 2.12: Aviso -MII: Final age distribtion. x-axis: [days], Left y-axis: [1000]

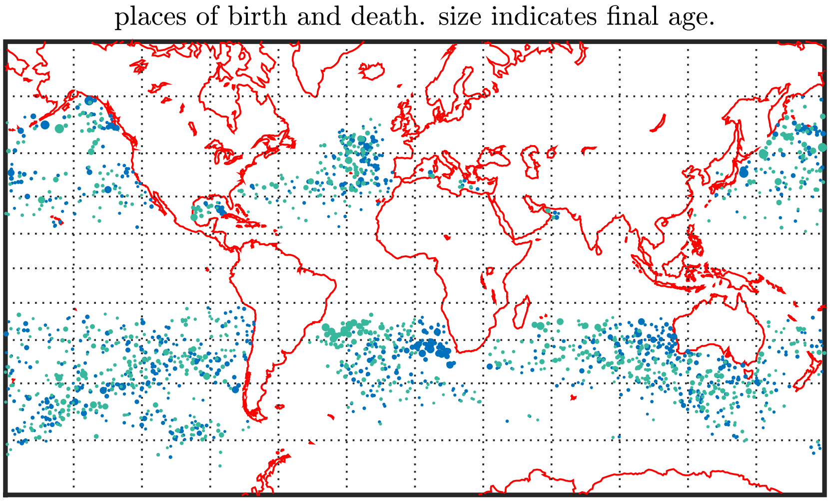

Figure 2.13: Aviso -MII: Births are in blue and deaths in green. Size of dots scales to age squared. Only showing tracks older than one year.

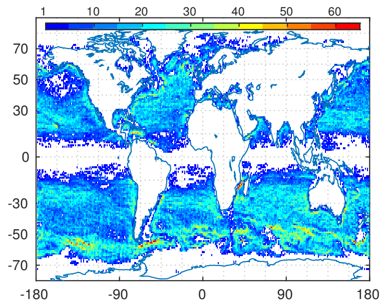

Figure 2.14: Aviso -MII: Total count of individual eddies per 1 degree square.

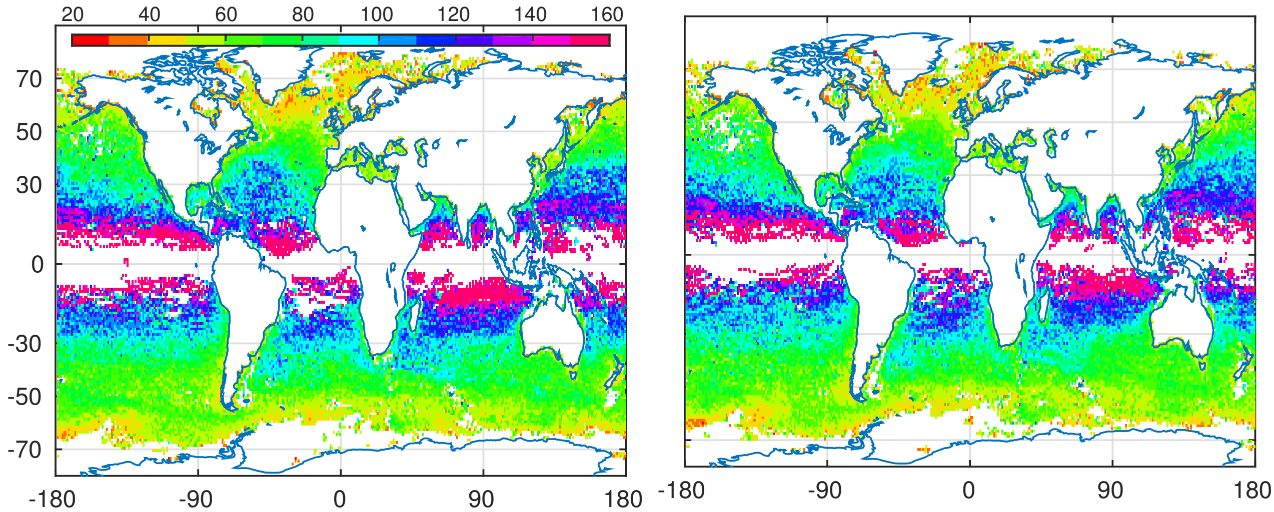

Figure 2.15: Aviso -MII: σ[km]

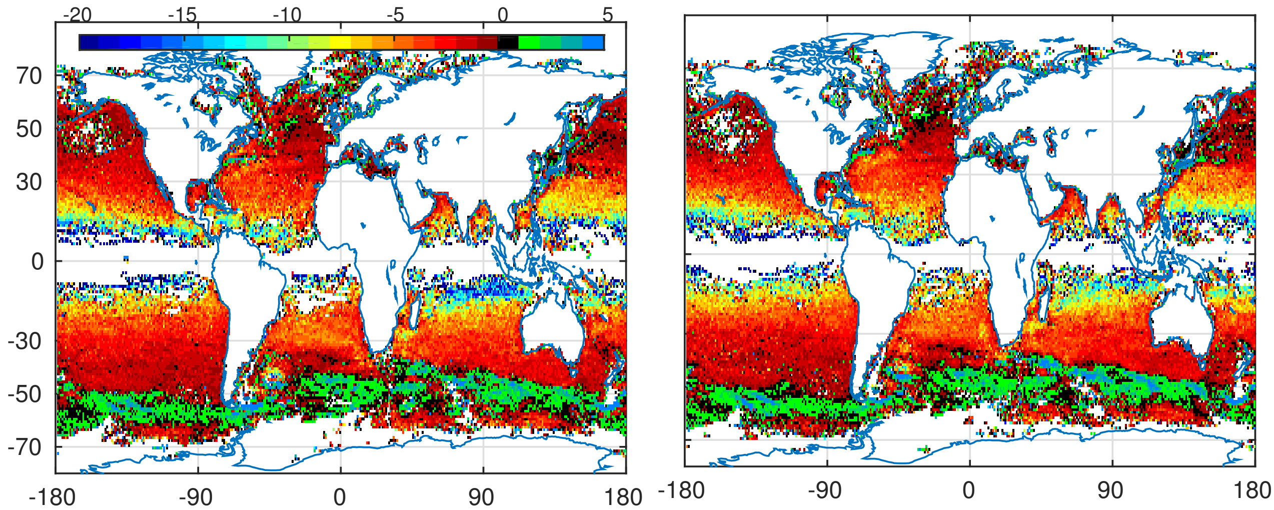

Figure 2.16: Aviso -MII: zonal translational speed [cm/s]

2.3 MII - 7 day time-step - POP

THE MODEL DATA delivers slightly more total tracks with a similar 2-fold dominance of cyclones over anti-cyclones (compare **????**). Similar to AVI-MII , very long tracks are fewer than via AVI-MI [2]. The regional pattern looks somewhat similar to the satellite patterns in terms of which regions feature the strongest eddy activity, with the exception of an unrealistic abundance of eddies right along the Antarctic coast where no eddies were detected for the satellite data likely due to sea ice and/or the inherent lack of polar data due to the satellites' orbit-inclinations.

[2] AVI-MI features 3000 tracks that are older than 400 days, while both MIImethods have only ~ 1000 of such.

THE more important difference between model- and satellite regional distributions is that the model results indicate significantly less eddy activity away from regions of strong SSH gradients, in the open ocean away from coasts and strong currents. The algorithm also detects hardly any eddy tracks in tropical regions (see **??**).

THE SCALE σ is generally smaller for the model-data-based analysis than for any satellite-based analyses, especially so in high latitudes.

WESTWARD DRIFT SPEEDS look regionally similar to those from satellite data (**????**). In the zonal mean their magnitude is below those from satellite (see **??**).

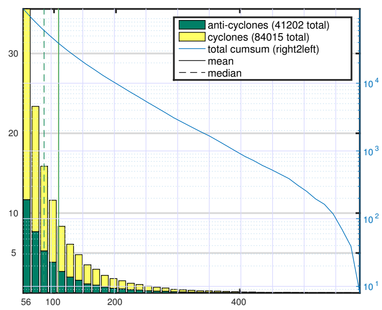

Figure 2.17: pop7-MII: Final age distribtion. x-axis: [days], Left y-axis: [1000]

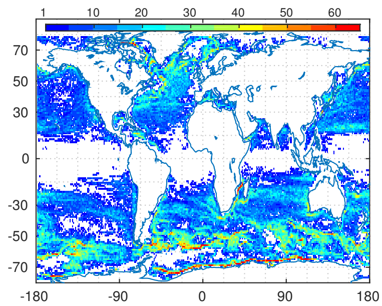

Figure 2.18: pop7-MII: Total count of individual eddies per 1 degree square.

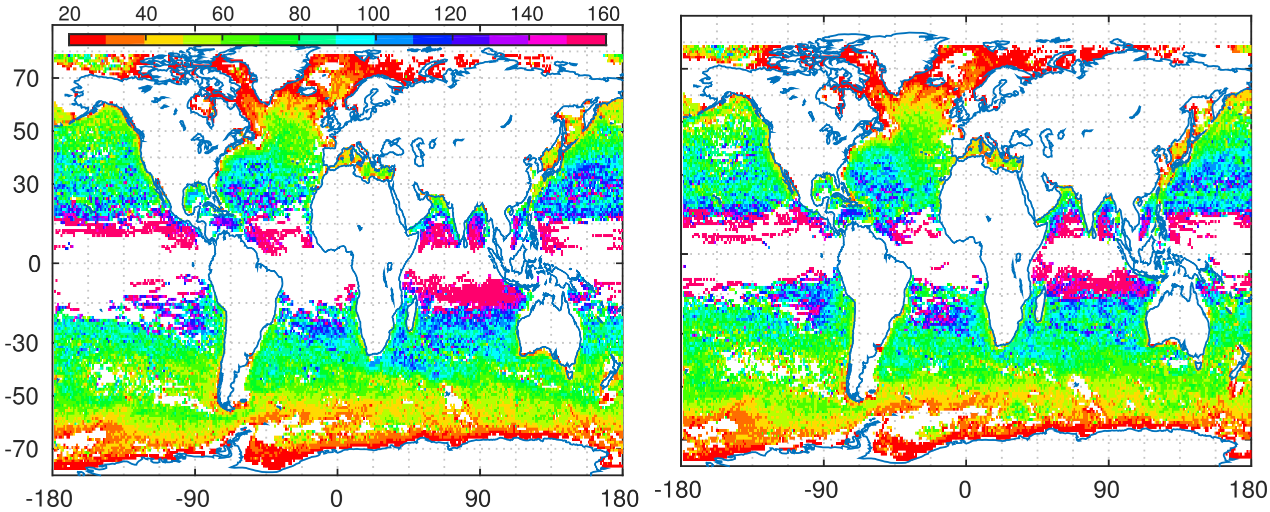

Figure 2.19: pop7-MII: σ[km]

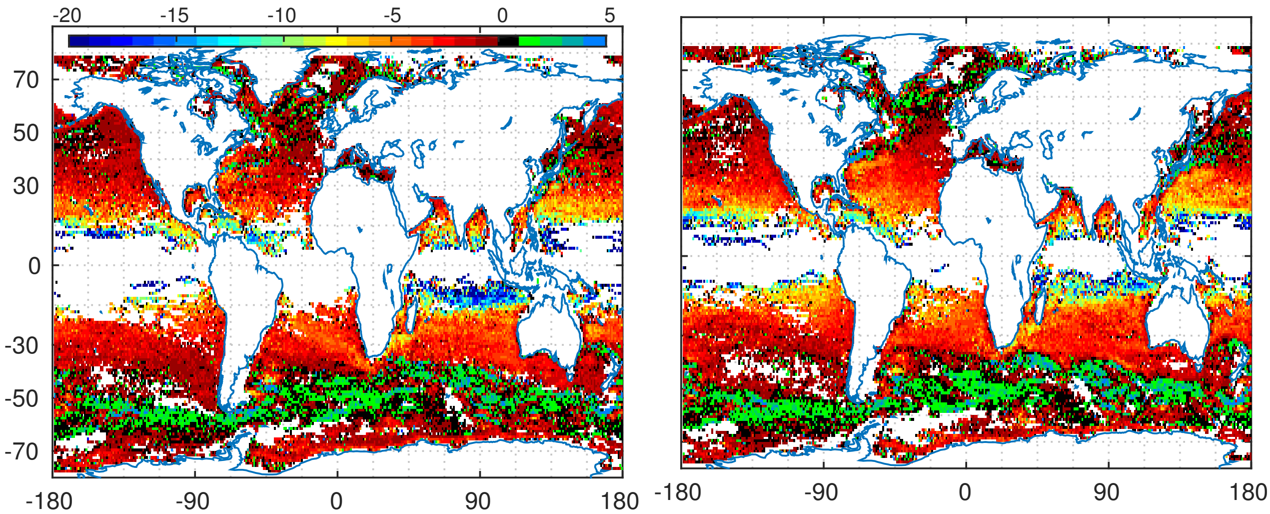

Figure 2.20: pop7-MII: zonal translational speed [cm/s]

2.4 MII - 7 day time-step - POP remapped to Aviso geometry

The model data

The scale σ

Westward drift speeds

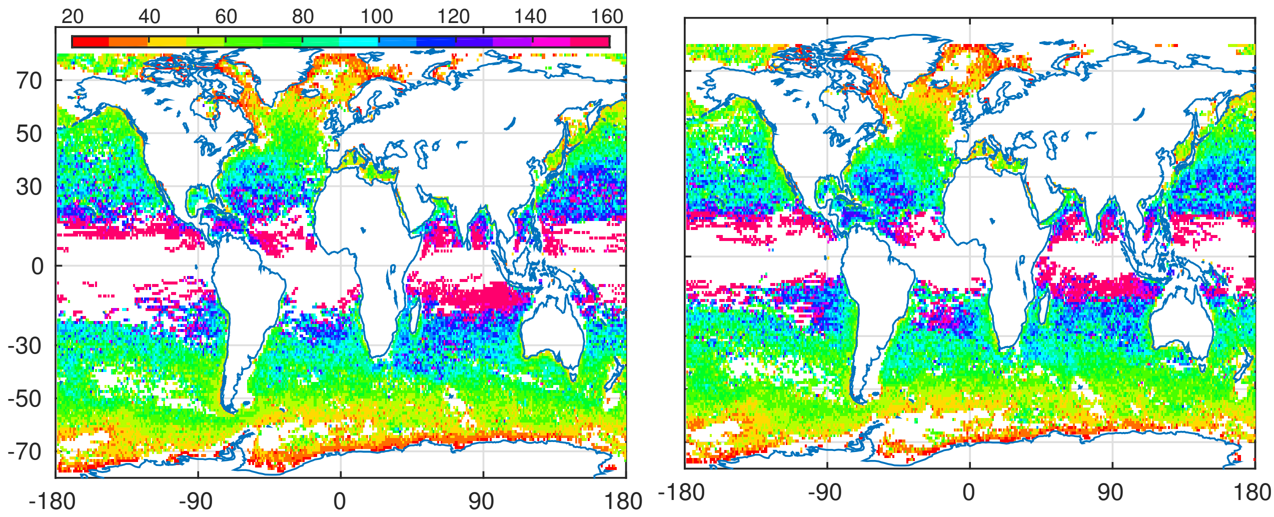

Figure 2.21: pop2aviso-MII: σ[km]

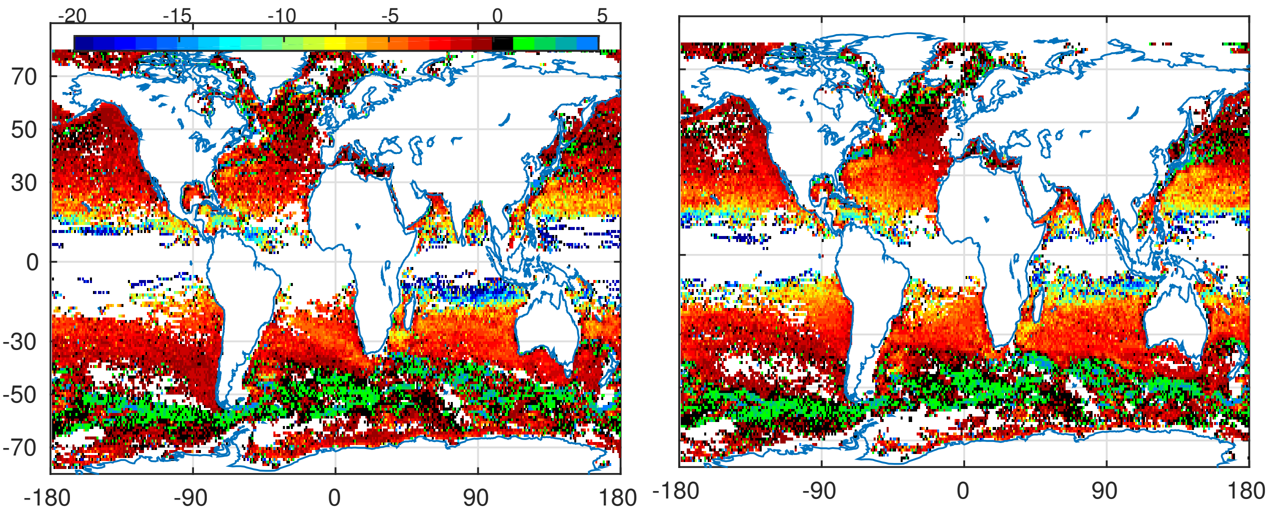

Figure 2.22: pop2aviso-MII: zonal translational speed [cm/s]

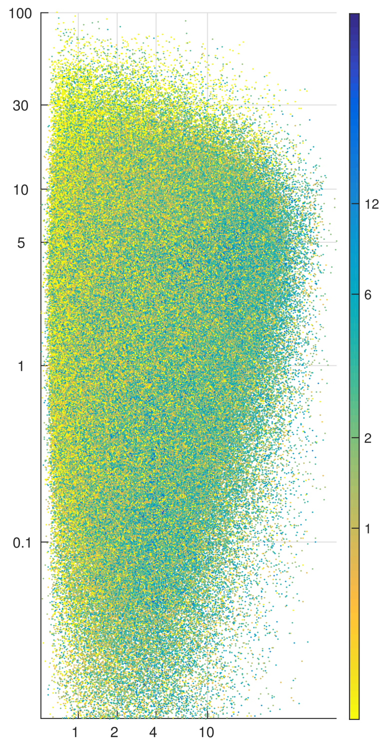

Figure 2.23: pop2aviso-MII: Small amplitude correlates with a short life and a broad translational speed spectrum. y-axis: translational speed [cm/s], x-axis: amplitude [cm], color: age [months] TODO: **use this as argument for 2cm contour step in pop2II**

2.5 MII - 1 day time-step - POP

TODO: **run is finished. Results will be looked at / interpreted next week**

2.5.1 TODO: net U

TODO:

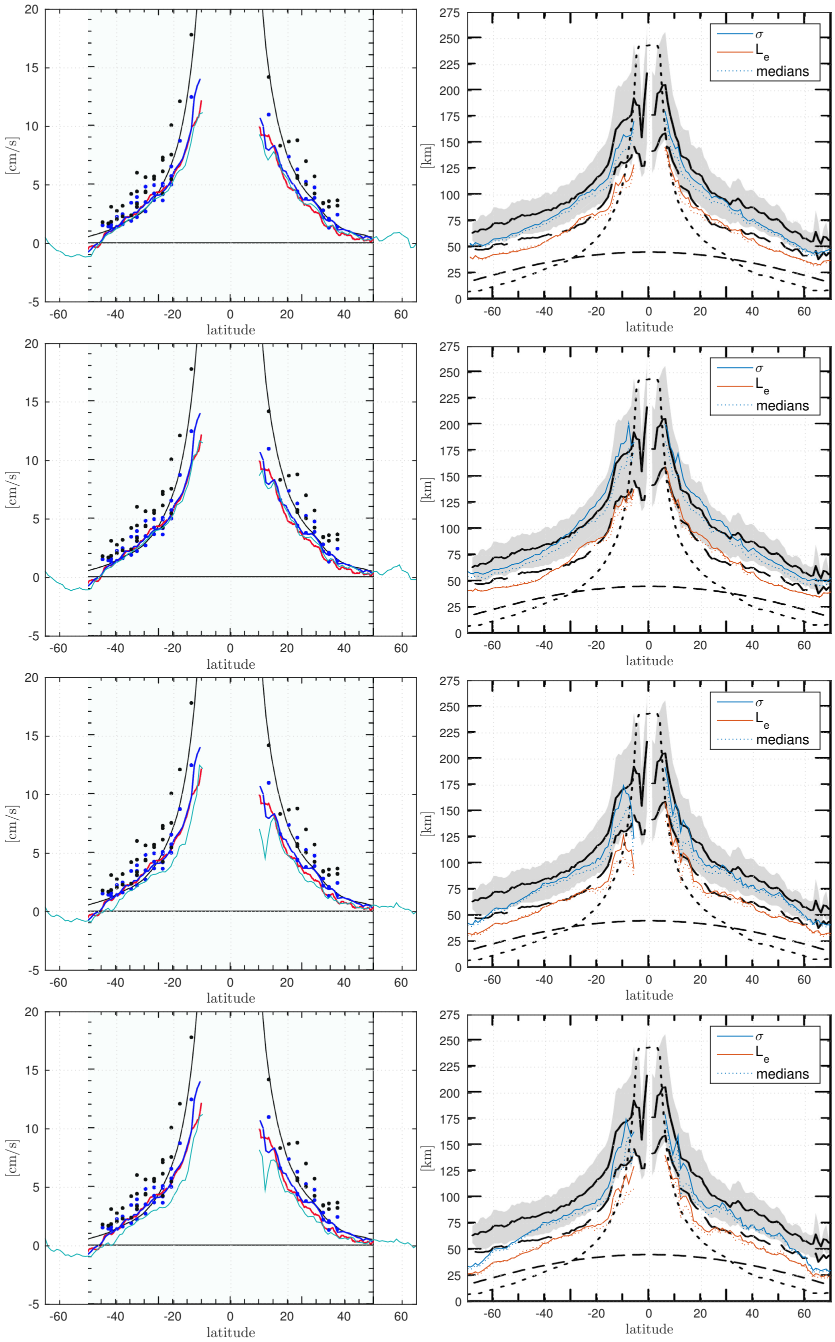

Figure 2.24: Left: Zonal-mean drift speed (cyan) fit to Fig 22 of (**?**) (Background). Right: σ and L_e fit to Fig. 12 of their paper. Dotted lines are medians instead of means. 1st row: AVI-MII , 2nd row: AVI-MI , 3rd row: pop2avi-MII , 4th row: POP-7day-MII . Note that for the very high latitudes ($> |60°|$) the contrast between model and satellite data is further intensified by the lack of satellite data (see **????**) in those regions (sea-ice / orbit inclinations). For a depiction without this effect see **??**.

3
Discussion

3.1 Lengths of Tracks

The most apparent difference between the results of the two detection-methods is the abundance of long-lived eddies resulting from the MI-method. This discrepancy must logically be caused by the two different contour-shape-testing procedures (**????**), since it is here where the main difference between the two methods' algorithms lies.

The MI-method is the more lenient one, as all it checks for, is whether the contour is of sufficiently compact form. The only shapes that are dismissed are long, thin elongated structures. This means that *e.g.* an eddy track can more easily [1] survive situations in which two eddies merge into one or those in which one is split into two or situations in which mean current gradients distort the vortex (see **??**). There could also be the situation in which an old, weak eddy fades, yet another one emerges in sufficient proximity. These two events would not even have to coincide at the exact same time, as long as some short-lived coherent structure, of which there is an abundance [2] at any given time-step throughout the world ocean, acted as a *bridge* to fill the gap.

The MII-method is conceptually different in that it is based on the assumption that a distinct coherent vortex need *per definition* to be more or less circular. It will therefor be more likely to regard *e.g.* the situation in which one eddy merges with another as a situation of 3 eddies in total; **two** that have just died to create **one** new one. The focus here is more on the propagation of distinct circular geostrophic

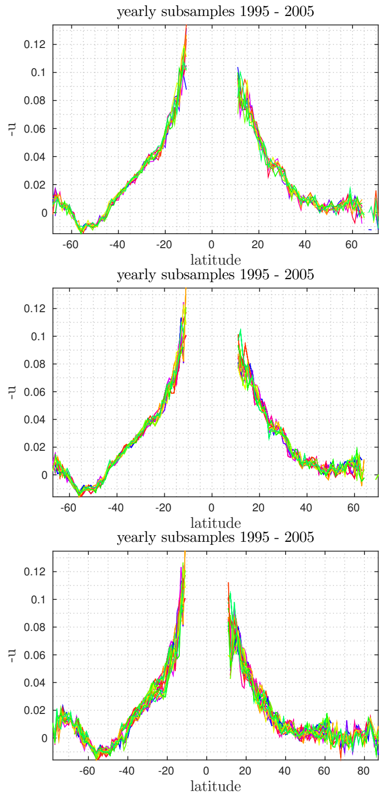

Figure 3.1: Each line represents zonal means of tracks that ended within one of the eleven years from 1995 to 2005. Top: AVI-MI . Middle: AVI-MII . Bottom: POP-7day-MII .

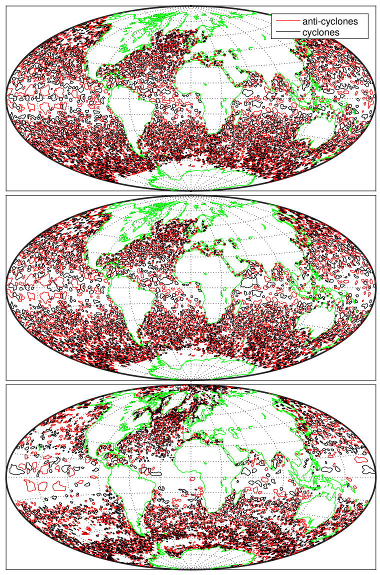

Figure 3.2: All contours that passed the filtering procedure for one exemplary time-step. Top: AVI-MI . Mid: AVI-MII . Bottom: POP-7day-MII .

[1] as long as the similarity-criterion is not violated.
[2] see **??**

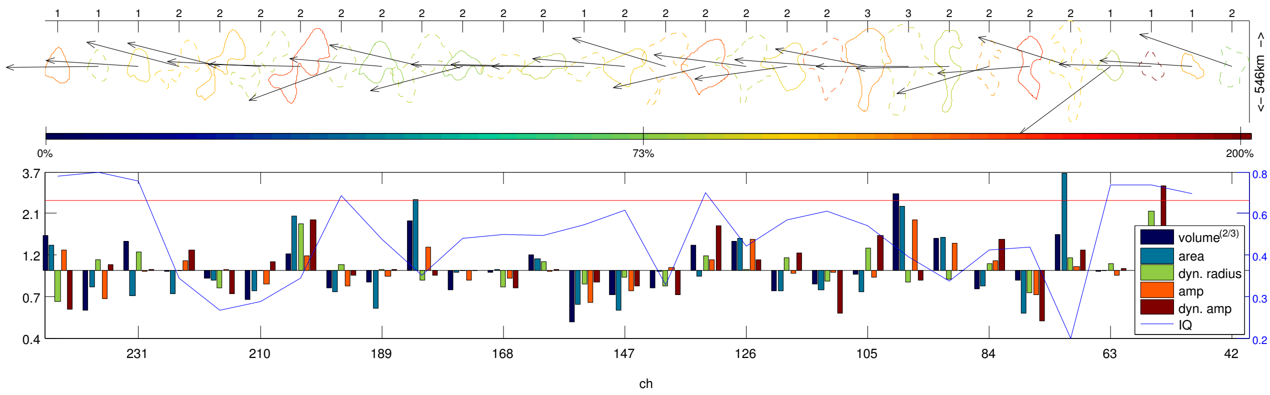

Figure 3.3: The MI-method. Top: Consecutive contours of one track. Colors indicate percentage of change of contour's area with respect to the prior time-step. Topmost horizontal axis shows the (rounded) factor of σ with respect to the local first baroclinic L_R. Vectors' lengths are proportional to the distance travelled with respect to the next time-step. Bottom: Blue graph shows the current IQ. Bars show the factors of change of respective parameters with respect to the prior time-step. X-axis are days since birth.

vortices whereas the focus in the MI-method is more general on coherent local depressions respective elevations in SSH (see **??**). It should be intersting to look at to which degree tracers found within tracked eddies remaine within the eddy over time (postponed for now). This could further clarify the hypothesis that the MI-method might be better at tracking water-mass advecting entities, with less jumps between bodies of water within one track. E.g. looking at temperature/salt at the eddy's core as a function of time **TODO: to conclusion?**

.

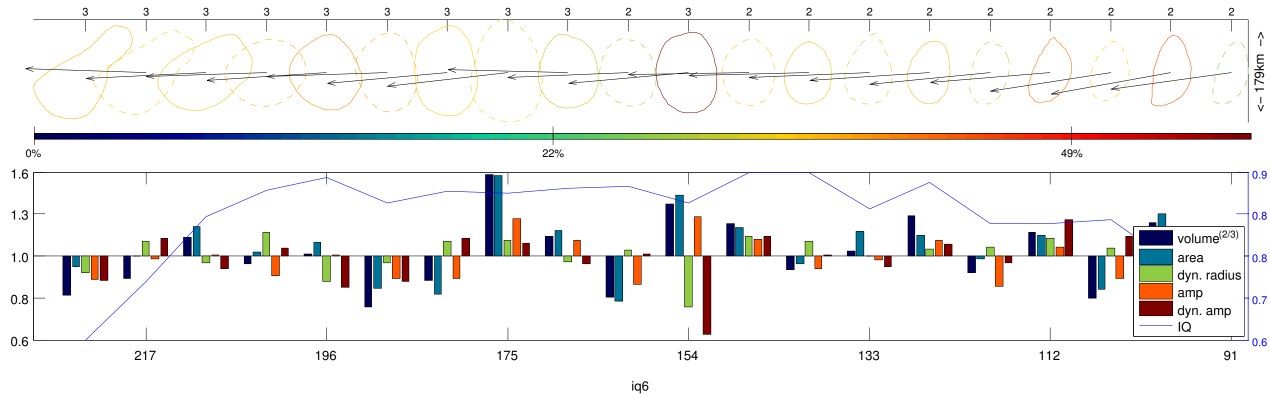

Figure 3.4: The MII-method (IQ-threshold at 0.6). (see **??**)

3.2 *Scales and the Effect of Downsampling*

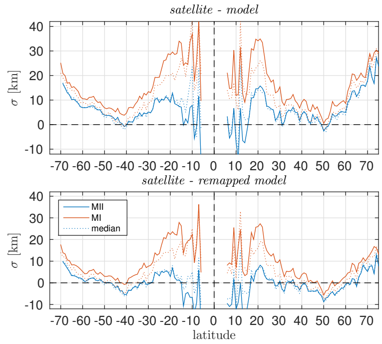

Figure 3.5: Differences in zonal mean σ between Aviso/POP and Aviso/downsampled POP. Means/Medians are built zonally over only those $1° \times 1°$-bins that feature data in both sets *i.e.* the intersection of $lat + 1i\ lon$ of both sets.

INTERESTINGLY, even in the AVI-MI results, the horizontal eddy scale σ differs from that presented by **?**. For latitudes $\gtrsim |25°|$ the zonal mean here is smaller than theirs while for low latitudes it is higher (see **??**). The reason for this discrepancy is suspected to stem from the special method by which σ is determined by our algorithm. As outlined in **??**, here σ is half the mean of zonal and meridional distances between the first two local extrema of the first derivative of interpolated 4th-order fourier fits to the SSH data around the eddy's CoV.

THE motivation to use fits instead of the SSH directly was on the one hand to avoid noise complicating correct determinations of the 2nd differential zero-crossings and on the other hand to tackle the problem of coarse resolution, especially so for high latitudes where σ seems to become as small as only twice the distance between data points. At this resolution the *Gaussian RMS width* of an eddy would amount to only 5 data points. Since σ is generally smaller in the higher-resolution POP-data analyses, we hypothesize that the scales by **?** are biased high for high latitudes. Question remains to what degree this bias is inherent to the Aviso product *i.e.* as a smearing effect from the interpolation of multiple coarse satellite data. Or whether it is attributable entirely to the particular method by which the diameter/area of the zero-vorticity contour is estimated.

STRONG zonal skewness suggests the existence of many small, potentially erroneous values that smear the distribution of drift speeds towards an unrealistically low mean. This effect appears to be relevant in *e.g.* the Souther Ocean, where the east-ward advection of eddies by the ACC results in a broad spectrum of drift speeds. The strong gradients in mean current also effect an abundance of eddy-merging and -splitting situations over relatively short periods of time. It is therefor difficult for the algorithm to keep track of sufficiently long-lived, coherent vortices. Especially so for large time-steps and a high age-threshold. Yet, if the minimum time-step is limited, as in the case of satellite data, a high age-threshold is necessary since short tracks with few data points in time are more likely to stem from erroneously matched contours that do not represent the actual track of a single vortex but instead represent other mesoscale noise that happened to feature sufficiently similar blobs popping in and out of existence at sufficient proximity to one another.

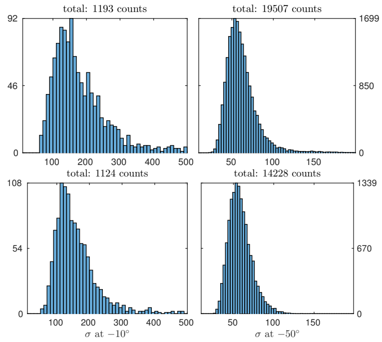

Figure 3.6: Eddy count at one point in time for one fully zonal 1°-bin. Top: AVI-MI . Bottom: AVI-MII . The tropical spectrum is broad yet with strong positive skewness *i.e.* oriented towards smaller scales. In high latitudes the standard deviation is smaller. The MImethod yields more large eddies.

WITH REGARD to the lower latitudes two important aspects need to be considered:

1. The analyses yield generally low eddy activity in the tropics. Hence the results are less robust in this region *a priori*.
2. The standard deviation in σ is particularly broad in the tropics (see **??**). As a matter of fact it appears as though there might be two different types of eddies. One type analogous to all high-latitude eddies and a new one of much larger scale. Because these larger eddies have generally low IQ-values they are filtered from the MIIanalyses, resulting in smaller tropical σ. Their more chaotic shape might, due to the different methods to determine σ, also have to do with why mean tropical σ is larger here than in **?**.

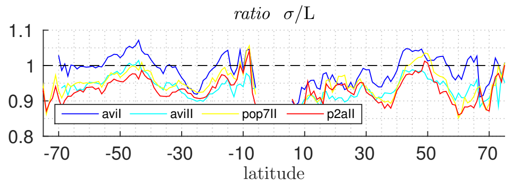

Figure 3.7: Ratios of σ to L (see **??**)

THE POP-7day-MII analysis yields somewhat simlilar σ for low latiudes [3], yet significantly smaller values for high latitudes. The question here therefor is whether this discrepancy is a result of the lower resolution of the satellite data *i.e.* that eddies are too small to be resolved by the Aviso product in high latitudes or whether it is attributable to the model data as in a systematic bias due to incomplete/poorly parameterized model physics. This question was the primary motivation for the pop2avi-MII -analysis. The idea here was to down-size the POP data to the geometry of the Aviso grid in order to test whether this would raise σ to that from the satellite results. **??** shows that the down-sampling did indeed decrease the discrepancy in σ to respective Aviso analysis, as long as those regions that are unique to either data set are excluded. Between ±25° and ±65° the difference is no larger than ±5 km. This came as a surprise because since σ stems from Fourier fits of SSH, we expected the original frequencies to be, at least to some extent, conserved in the

[3] Note that due to the lack of tropical eddies the estimates of σ are rather uncertain for the POP analyses.

down-sampled data.

3.3 *Profiles*

The MIdetection method a priori assumes that an eddy is more or less detected at its asymptotic *floor i.e.* in the case of an AC at the *foot of the mountain*. The idea of the IQ-based method on the other hand is to assume that the situation of a single well-defined eddy sitting on an otherwise smooth, flat sea surface, which would be necessary for the contour algorithm to find a closed contour describing the outermost perimeter of said single vortex, is unrealistic. Instead the approach is to look for distinct, sufficiently circular *caps* of SSH-hills/valleys that consistently *wade* through all other weaker geostrophic noise surrounding it.

TODO: why gaussian or quad? Read ??

TODO: explain ????

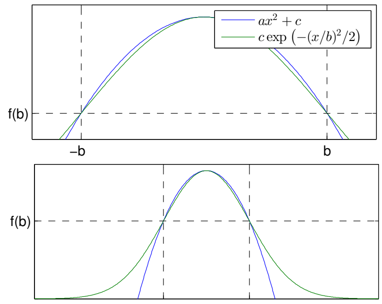

Figure 3.8: The upper part of a Gaussian profile can appear similar to a quadratic one. **TODO: ref to here**

3.4 *Drift Speeds*

Zonal mean drift speeds of all Aviso results agree well with those presented by **?** (see **??**), suggesting that the tracking procedures are relatively robust for both the MIand MIImethods.

The POP-7day-MII results yield generally smaller magnitudes of u. The apparent drop in magnitude at $\sim$ 12°N is most likely due to erroneous inter-time-step eddy-associations. In that region, the combination of extreme sparsity of results, large time-step, large σ, low amplitude and high (theoretical) drift speed make robust determinations of u practically impossible. Yet the tendency for lower magnitudes in u, albeit less stark, is also true for higher latitudes. The zonal drift speeds are calculated via gradients of *polyfits* to the CoV-locations on the surface of a spherical earth. This method was tested thoroughly and its robustness is further validated by the fact that the weaker u remains approximately the same after down-sampling for the pop2avi-MII run.

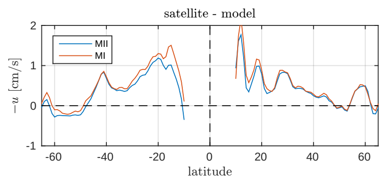

Figure 3.9: AVI-MI /AVI-MII minus POP-7day-MII of zonal drift speed means.

From equation (**??**) we know that at first approximation (planetary lift)

$$u \sim \beta \left(\frac{NH}{f_0} \right)^2 \tag{3.1}$$

Since β, H and f should have been set realisticaly in POP, it appears that the, evidently unrealistic, drift speeds in the model results stem from an unrealistic or poorly resolved (only 42 vertical layers in POP) density stratification $\frac{\partial \rho}{\partial z}$.

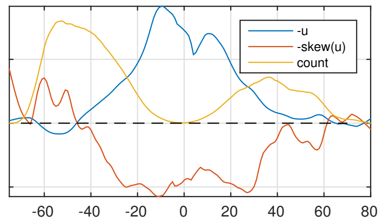

Figure 3.10: Skewness (red) of $-u$ for AVI-MI . The spectrum leans towards high westward values in low latitudes. In the ACC the distribution reverses indicating the existence of sporadic events of strong eastward advection by the mean flow. (Note: Everything normalized to fit all in one frame.)

3.5 *POP-1day-MII-Southern-Ocean*

TODO: run is finished. Results will be looked at / interpreted next week

4
Conclusion

4.1 POP-1day-MII-Southern-Ocean

TODO:

4.2 things to do bla

TODO: more data, depths, surface intensified, upper layer

TODO:

Further study in refining this structure is expected, and the refined structure can serve as a benchmark for numerical models where mesoscale eddies are explicitly resolved. In addition, the generation mechanism for this universal structure remains unknown; thus, exploring such mechanism may bring new excitement to eddy research. ?

TODO: 3d structure still mystery

TODO: H/f contours

TODO: tracers AC/C diff

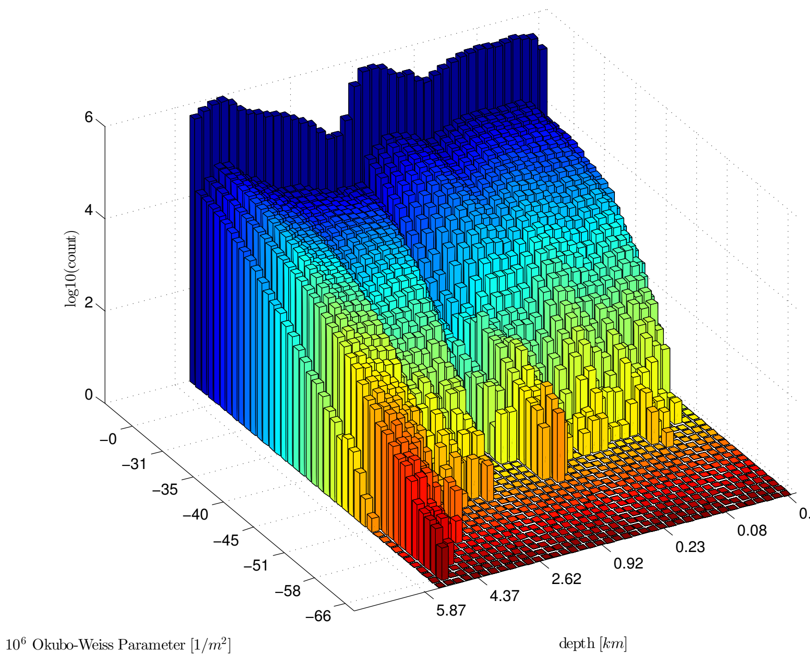

Figure 4.1: Histogram of global $\mathrm{O_w}$ as a function of depth calculated from POP $\boldsymbol{u}$-data. The idea was to find the surface $z_{ow}(y,x)$ of minimum $\mathrm{O_w}(z,y,x)$ and then use that depth as the depth to take the mean current from (see **??**). The maximum tends to be at the ocean floor which led to the conjecture that the numerical implementation of $\mathrm{O_w}$ might have been erronuos. Further applcation was hence abandoned.

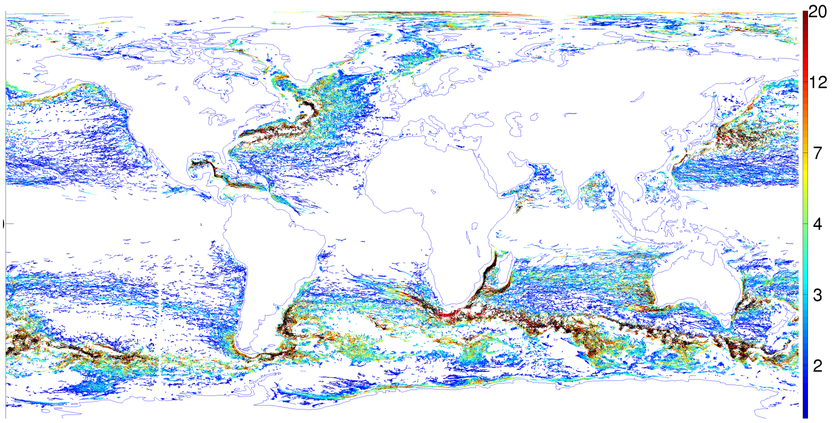

Figure 4.2: Amplitude [cm] (w.r. to contour). Tracks are from very early POP test-runs.

TODO: bibtex warnings
TODO: abc
TODO: units 2 siunitx
TODO: flatten some complex pdfs
TODO: check overlaps of figs
TODO: [box:bla] in toc?